Geomechanics and Engineering, *Vol. 29, No. 3 (2022) 291-300*
https://doi.org/10.12989/gae.2022.29.3.291

Numerical evaluation of surface settlement induced by ground loss from the face and annular gap of EPB shield tunneling

Jun-Beom An[a], Seok-Jun Kang[b], Jin Kim[c] and Gye-Chun Cho*

Department of Civil and Environmental Engineering, Korea Advanced Institute of Science and Technology, 291 Daehak-ro, Yuseong-gu, Daejeon 34141, Republic of Korea

(Received December 17, 2021, Revised February 22, 2022, Accepted March 9, 2022)

Abstract. Tunnel boring machines combined with the earth pressure balanced shield method (EPB shield TBMs) have been adopted in urban areas as they allow excavation of tunnels with limited ground deformation through continuous and repetitive excavation and support. Nevertheless, the expansion of TBM construction requires much more minor and exquisitely controlled surface settlement to prevent economic loss. Several parametric studies controlling the tunnel's geometry, ground properties, and TBM operational factors assuming ordinary conditions for EPB shield TBM excavation have been conducted, but the impact of excessive excavation on the induced settlement has not been adequately studied. This study conducted a numerical evaluation of surface settlement induced by the ground loss from face imbalance, excessive excavation, and tail void grouting. The numerical model was constructed using FLAC3D and validated by comparing its result with the field data from literature. Then, parametric studies were conducted by controlling the ground stiffness, face pressure, tail void grouting pressure, and additional volume of muck discharge. As a result, the contribution of these operational factors to the surface settlement appeared differently depending on the ground stiffness. Except for the ground stiffness as the dominant factor, the order of variation of surface settlement was investigated, and the volume of additional muck discharge was found to be the largest, followed by the face pressure and tail void grouting pressure. The results from this study are expected to contribute to the development of settlement prediction models and understanding the surface settlement behavior induced by TBM excavation.

Keywords: EPB shield TBM; excessive excavation; face pressure; ground loss; surface settlement; tail void grouting pressure

1. Introduction

Tunnel boring machines (TBMs) have been extensively adopted for tunnel construction in urban areas because they mechanically excavate tunnels, generating less vibration, noise, and dust than the conventional blasting methods. Although ground deformation must be strictly limited during urban tunneling, the ground on which the TBMs are being applied has been expanding; therefore, an earth pressure balanced (EPB) shield TBM was proposed to limit the induced settlements. The EPB shield TBM can restrain the surface settlement through continuous and repetitive support after excavation. It can secure the pressure balance between the total earth pressure and face pressure, because of the presence of a pressurized muck inside the chamber. The parameters triggering the surface settlement vary and have been studied using several methods. Tunnel design factors such as the diameter and depth of the tunnel (Melis *et al.* 2002, Chakeri *et al.* 2013), various ground properties such as the elastic modulus, cohesion, and unit weight (Selby 1988, Golpasand *et al.* 2018, Kim *et al.* 2018a), and the operational factors such as face pressures and steering gap slurry pressures (Lambrughi *et al.* 2012, Comodromos *et al.* 2014), tail void grouting pressure, the amount of backfills and injection point (Suwansawat and Einstein-2007, Kim *et al.* 2018b), and other mechanical data from TBMs (Goh and Hefney 2010, Kim *et al.* 2020), are all related to unavoidable gaps or stress imbalances. Among these factors, the operator can regulate the support pressure on the tunnel face, along the shield skin, and along the cylindrical excavated surface beyond the segment linings. However, surface settlements that are unrelated to the pressure balance can be caused by direct ground loss such as excessive excavation. If the operator encounters mixed ground, the soft region can be excavated without much support from the face pressure. The increased muck discharge directly contributes to the surface settlement.

In this study, parametric studies using numerical methods were conducted to evaluate the contribution of improper mucking by excessive excavation to the surface settlement, in addition to the contribution of ground stiffness, face pressure, and tail void grouting pressure. First, a numerical model for ordinary excavation sequences was constructed and validated by comparing the results with those reported in the literature. The excessive excavation was then simulated using a theoretical sliding surface analysis method. It is expected that the order and amount of contribution to the surface settlement can be applied to the

*Corresponding author, Professor
E-mail: gyechun@kaist.ac.kr
[a]Ph.D. Student
[b]Ph.D. Student
[c]Ph.D. Student

ISSN: 2005-307X (Print), 2092-6219 (Online)

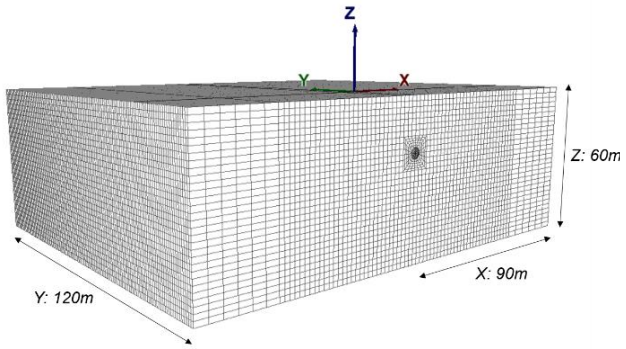

Fig. 1 Schematic of a finite difference mesh

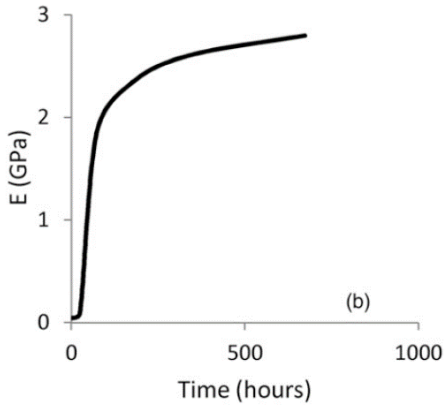

Fig. 2 Hardening behavior for mortar grout pressurized in the tail void (Comodromos *et al.* 2014)

development of settlement prediction models and help to understand the settlement behavior induced by EPB shield TBM excavation in a realistic view.

2. Development of the numerical model

A numerical analysis was carried out based on the finite difference method (FDM) using the commercial software FLAC3D developed by Itasca.

2.1 Modeling of the ground

The size of the domain should be determined to describe the ground in accordance with an infinite medium, such that the error due to the reaction from the boundary is negligible. The minimum dimensions were selected to be in the range of (H+3D) to 2(H+4D) for the mesh length, 3H to 2(H+4D) for the mesh width, and (H+4D) for the mesh height, where H is the depth of the tunnel axis and D is the tunnel diameter (Lambrughi *et al.* 2012). In this manner, the domain size was 120 m in the longitudinal direction of excavation, 90 m from the tunnel axis in the transverse direction, and 60 m for the mesh height (Fig. 1). The ground was constructed using zone elements, and the roller boundary condition was applied. The nodes at all sides of the model were fixed in the horizontal directions, while the nodes at the base of the model were fixed in the vertical directions. The initial condition of the ground was calculated iteratively until the mechanical ratio between the unbalanced forces reached below 1e-05 after the ground properties and gravitational force were designated.

2.2 Modeling of the structural elements

Structures such as EPB shield TBM, lining segments, and backfill grouts at the tail void were simulated using shell elements with a linear elastic model (Comodromos *et al.* 2014, Moeinossadat and Ahangari 2019). The shield was assumed to have no tapering or steering gaps. In addition, the zone elements overlapped the shell elements for lining segments and grouts to consider the deformation in the thickness direction.

2.3 Modeling of the face support

The face support was simulated by applying stress in a direction normal to the nodes on the tunnel face. Although the horizontal earth pressure experienced by the shield face differed from the crown to the bottom, the face pressure was simulated with an identical value estimated from the center of the tunnel. The face pressure is described using the FPR parameter, which is the ratio between the face pressure and horizontal total earth pressure at rest on the tunnel face.

$$\mathrm{FPR} = FP/\sigma_y = FP/(K_o \cdot \sigma_z' + u) \quad (1)$$

where, the FP is the face pressure.

2.4 Modeling of the tail void grouting

The grout pressurized on the tail void was simulated to be hardened with time, similar to the experimental data plotted in Fig. 2 which shows the representative hardening behavior (Comodromos *et al*. 2014).

For simpler and faster simulation, grout hardening was discretely simulated in this study. The average advance of the shield was assumed to be 10 rings per day. 2, 3, 20, 40, 55, 65, 72, 74, 76, 78, 80, and 81% of the completely hardened modulus was applied at each of the five rings after injection. The grout injection pressure on the tail void was applied to the excavated surface uniformly in a normal

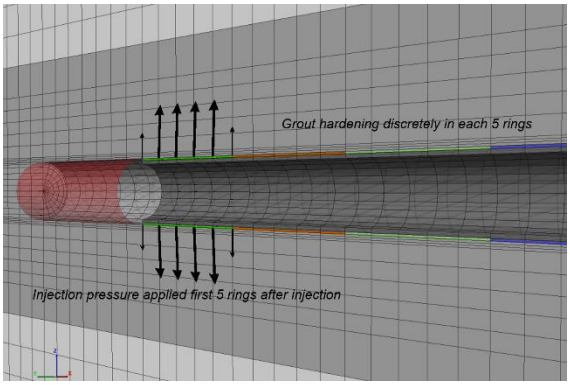

Fig. 3 Schematic diagram of grout injection in tail void

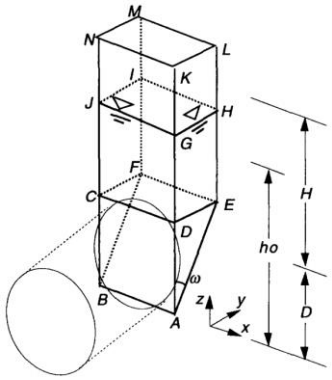

Fig. 4 Sliding mechanism (Anagnostou and Kovari 1994)

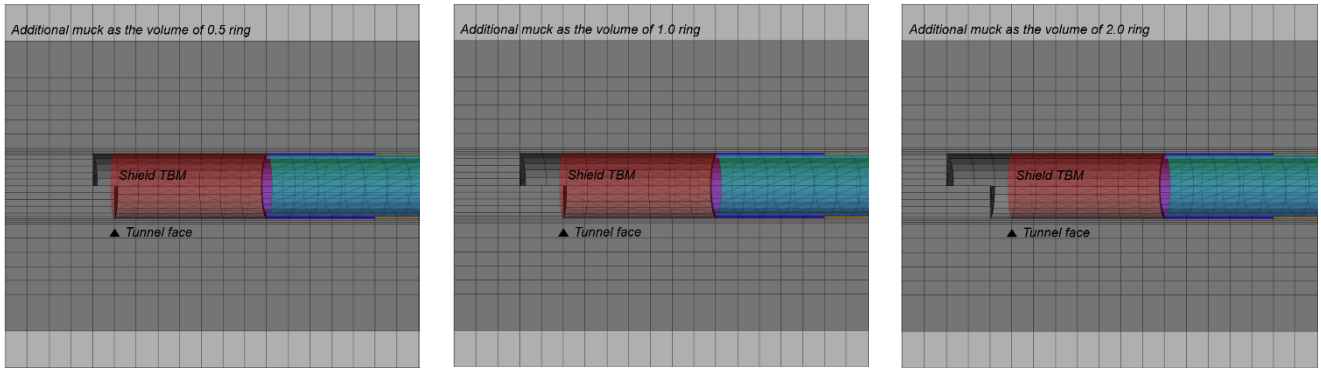

(a) Volume of 0.5 ring (b) Volume of 1.0 ring (c) Volume of 2.0 rings

Fig. 5 Schematic diagram of excessive excavation controlled by the volume of additional muck discharge

direction for up to five rings after injection and the initial setting time of the grouts was assumed to be 12 h (Fig. 3).

The injection pressure applied on the tail void should be 100–200 kPa larger than the face pressure (KDS 2016), and is recommended in a range that does not cause heaving of the ground surface. Thus, the grout injection pressure was approximately 100 kPa greater than the face pressure. This pressure is described using the backfill injection pressure ratio (BPR), which is the ratio between grout injection pressure and total horizontal earth pressure at rest on the tunnel face.

$$\text{BPR} = BP/\sigma_y = BP/(K_o \cdot \sigma_z' + u) \tag{2}$$

where, the BP is the backfill grouts injection pressure.

2.5 Modeling of the excessive excavation

As the face pressure is lower than the horizontal earth pressure, ground loss occurs owing to an imbalance in the tunnel face. The operator controls the face pressure with the inclination or rotation of the screw conveyor to obtain a proper advance rate. In this manner, an additional muck can be accepted. However, excessive excavation may occur if the face pressure does not work properly owing to the unpredictable occurrence of mixed and soft ground or operational error. In the numerical simulation, excavation was performed by nulling the elements. Thus, excessive excavation beyond the tunnel face cannot be adequately described. In this study, excessive excavation was simulated with an accident in consideration by applying the sliding mechanism of soil, because the support would not work properly (Fig. 4, Anagnostou and Kovari 1994).

The inclination of the sliding wedge ω is determined by the internal friction angle ϕ, following Rankine's active wedge.

$$\omega = \frac{\pi}{4} - \frac{\phi}{2} \tag{3}$$

Therefore, the excessive excavation was simulated by nulling the elements beyond the shield face as 0.5, 1.0, and 2.0 times the ring volume by considering the sliding angle and discrete elements (Fig. 5). Therefore, the face pressure was not applied to the nullified zone right in front of the shield face. The calculation of excessive excavation was executed in 1000 steps.

2.6 Modeling of the TBM excavation process

The tunneling process of the EPB shield TBM was iteratively carried out in sequence by nulling the elements corresponding to the unit advance (a ring span), loading the face pressure, creating lining segments, and backfill grouts with injection pressure (Fig. 6). The face pressure on the former tunnel face was eliminated as the shield advanced. Then, the excavation sequences were simulated from the point of shield TBM takeoff, so the structural elements were

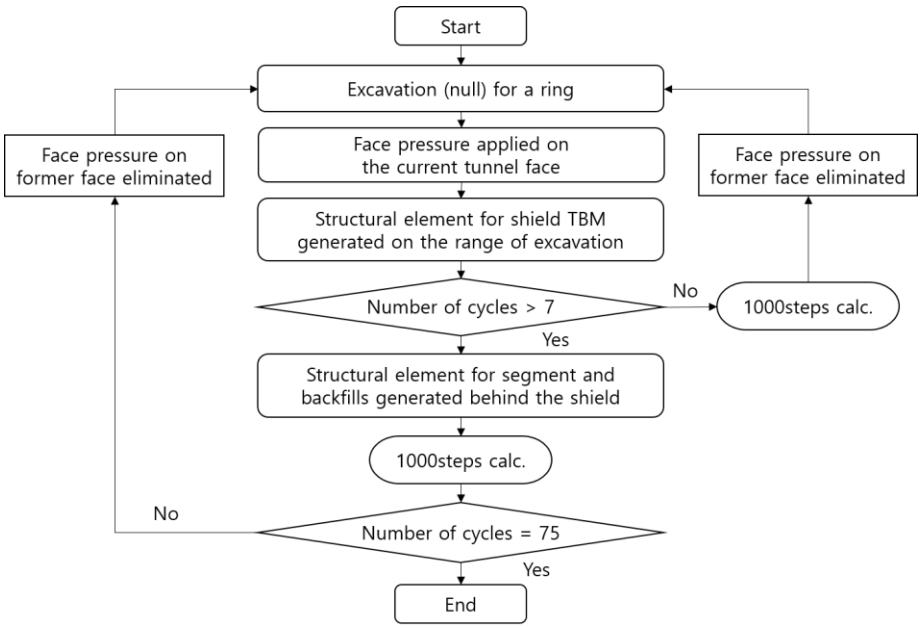

Fig. 6 Simulated EPB shield TBM excavation sequences in numerical modeling

not created until the TBM advanced as its own length (at the seventh cycle). Every tail void grouting was achieved by simultaneous injection. Every single advance required 1000 steps of calculation. The command 'step' was applied to simulate the continuous support. The tail void grouts had an elastic modulus that increased with discrete values, so if we used the command 'solve', it might collapse at the lower modulus range right after the shield. Because the unbalanced force ratio after every 1000 steps was lower than 1e-05, implying the rule of thumb convergence at FLAC3D, the command 'step' would be appropriate. The number of steps was determined empirically as the reasonably small value of 1000 (Chakeri *et al*. 2013, Hasanpour 2014, Moeinossadat and Ahangari 2019).

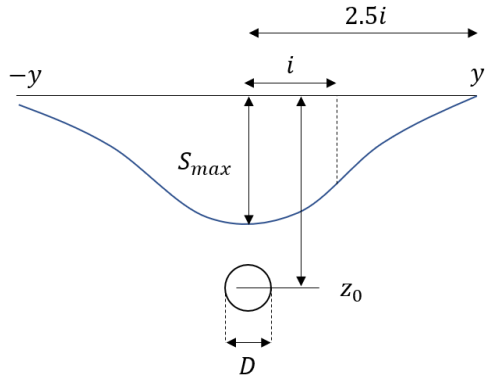

Fig. 7 Surface settlement profiles of Gaussian form

3. Validation of the numerical simulation

3.1 Definitions of surface settlement phenomena

The settlement resulting from the tunnel construction showed a settlement trough above the tunnel. The transverse settlement trough has been demonstrated to follow a Gaussian, distribution curve (Peck 1969, O'Reilly and New 1982, Sugiyama *et al*. 1999). The Gaussian distribution curve is plotted using the equation:

$$S = S_{max} \cdot exp\left(\frac{-y^2}{2i^2}\right) \tag{4}$$

where S is the settlement trough at the point y, S_{max} is the maximum settlement at the tunnel centerline, y is the distance from the tunnel centerline, and the i is the distance from the tunnel centerline to the inflection point of the curve (Fig. 7). The inflection point i can be assumed, with respect to the depth of the tunnel z_0 and trough width parameter K (O'Reilly and New 1982), as

$$i = Kz_0 \tag{5}$$

Mair and Taylor (1997) proposed the value of parameter K as 0.5 for clays and 0.35 for sands or gravel based on field data. The volume (unit area) of the settlement trough (V_S) was deduced by integrating Eq. (4). The volume loss (V_L) was defined as the ratio between the unit excavation area and the unit area of the settlement trough:

$$V_S = \sqrt{2\pi} i S_{max} = V_L \cdot \left(\frac{\pi D^2}{4}\right) \tag{6}$$

3.2 Validation: Tehran subway line 7

3.2.1 Validation setup

The numerical model was validated by simulating the Tehran subway line 7 construction performed with an EPB shield TBM (Moeinossadat and Ahangari 2019). The Tehran subway line 7 connects eastern Tehran to north-western Tehran. The target site for investigating the surface settlements was located at the station of 12 + 600 to 12 + 710 m. The depth

Table 1 Ground properties for validation of numerical model (Moeinossadat and Ahangari, 2019).

	Type (BSCS)	Thickness [m]	Density [kg/m^3]	Cohesion [kPa]	Internal friction angle [degree]	Elastic modulus [MPa]	Poisson's ratio
Layer 1	Fill	1.2	1,900	29	35	15	0.30
Layer 2	ML, CL	8	1,900	40	27	30	0.35
Layer 3	GML, GCL	11.6	1,900	30	35	80	0.27
Layer 4	GWM, GML	Base	1,900	20	38	100	0.27

*BSCS. ML: Silt, CL: Clay, GML: Silt with gravel, GCL: Clay with gravel, GWM: Well graded silty gravel

Table 2 Properties of structural elements (Moeinossadat and Ahangari 2019)

	Elastic modulus [GPa]	Poisson's ratio	Density [kg/m^3]	Shear modulus [GPa]
Shield	200	0.25	7,840	80
Segment	27	0.2	2,400	11.25
Grout	1	0.25	1,200	0.4

of the tunnel was 20.8 m. The geological and geotechnical properties of the target site are listed in Table 1. This ground had four layers composed of clay, silt, and gravel, which have an elastic modulus of up to 100 MPa. There was no water seepage at this site. The EPB shield TBM applied at this site had a diameter of 9.2 m, shield length of 9.0 m, external diameter of segment of 8.85 m, ring span of 1.5 m, and a ring thickness of 0.35 m. For the convenience of geometry formation, the external diameter of the segment was selected to be 8.90 m. The properties of the shield, lining segment, and backfill grout are listed in Table 2.

Operational factors such as the face pressure or grout injection pressure have not been confirmed in the literature. Various methods have been proposed for the design of the face pressure range (Davis *et al.* 1980, Anagnostou and Kovari 1996, Carranza-torres 2004). In this study, the face pressure was controlled within the range from Rankine's active pressure to the earth pressure at rest as a simplified view

$$FP_{max} = (1 - sin\phi') \cdot \sigma_z' + u \quad (7)$$

$$FP_{min} = \frac{1 - sin\phi'}{1 + sin\phi'} \cdot \sigma_z' + u \quad (8)$$

Therefore, the maximum face pressure (FP_{max}) has an FPR value of 1.0, and the minimum face pressure (FP_{min}) has an FPR value of approximately 0.6 at dry ground. Chakeri et al. (2013) executed a numerical study involving an identical site with a lower face pressure value of up to 88 kPa. Thus, the validation of the numerical model was performed using FPR 0.6. The BPR was selected as 1.1 to consider the construction standard.

3.2.2 Validation: results

A settlement trough was created for the numerical model validation, as shown in Fig. 8. The surface settlement had accumulated and converged with the iteration of the shield advance, as shown in the longitudinal settlement trough (Fig. 8(a)). The transverse settlement trough shown in Fig. 8(b) followed the Gaussian distribution curve and had an inflection point 6.5 m away from the tunnel center. The trough width parameter K was 0.31, which was close to the ordinary value for gravel or weathered rock. The maximum surface settlement of this target section was 6.95 mm in the numerical experiments, and it was nearly identical to the measured field-value of 6.9~7.1 mm. Therefore, the numerical model developed in this study can be accepted as valid.

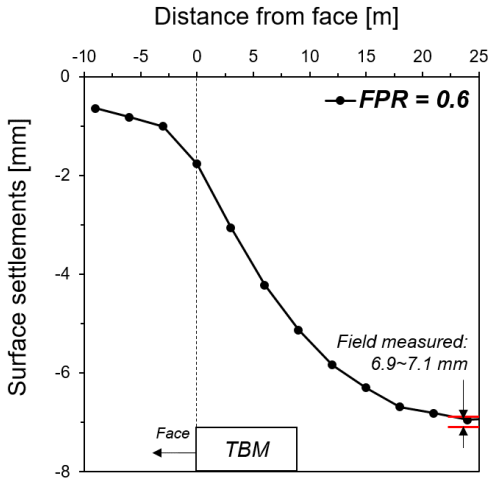

(a) Longitudinal settlement trough

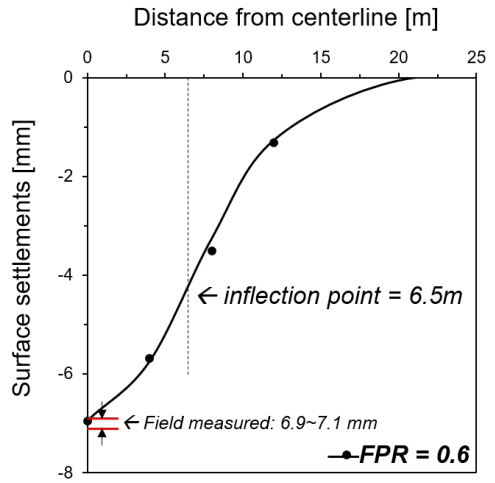

(b) Transversal settlement trough

Fig. 8 Surface settlement trough for validation of numerical model

Table 3 Properties of structural elements for parametric studies

	Elastic modulus [GPa]	Poisson's ratio	Density [kg/m^3]	Shear modulus [GPa]
Shield	200	0.25	7,840	80
Segment	35	0.2	2,500	14.6
Grout	2.8	0.25	2,200	1.12

Table 4 Ground properties for parametric studies.

	Type	Thickness [m]	Density [kg/m^3]	Cohesion [kPa]	Internal friction angle [degree]	Elastic modulus [MPa]	Poisson's ratio
Layer 1	Fill	4.0	1,800	5	26	18	0.33
Layer 2	WS	4.0	1,900	20	30	44	0.32
Layer 3	WR	4.0	2,100	30	33	100	0.30
Layer 4	SR	16.0	2,500	140	37	2,000	0.28
Layer 5	HR	32.0	2,800	1,000	45	8,000	0.25

*WS: weathered soil, WR: weathered rock, SR: soft rock, HR: hard rock

4. Parametric studies

4.1 Test conditions

With the same numerical domain, the depth of the tunnel was fixed at 20 m. The EPB shield TBM applied in these parametric studies had a diameter of 3.6 m, shield length of 8.4 m, ring span of 1.2 m, and the external diameter of segment was 3.4 m, which aimed the small-sectional utility tunnels. The properties of the shield, lining segment, and backfill grout have been listed in Table 3. The properties of the EPB shield TBM followed the machine manufactured by Kawasaki, and the properties of the segment corresponded to concrete grade C40/50 (Comodromos *et al.* 2014). The properties of grout differed with the field and were determined by ordinary values.

Geometric sketch of the representative ground with five layers is shown in Fig. 9. The geotechnical properties of the representative ground have been presented in Table 4. The parametric studies for the ground type were performed by simulating each type of rock for the tunneling layer (fourth layer) from the representative ground: the weathered rock (WR), soft rock (SR), and hard rock (HR). The rock medium was chosen as the target ground because the EPB shield TBM tunneling is applied with enough depth in general (20 m in this study). When the properties of the fourth layer were substituted with those of the aimed ground types, the density was not changed to reasonably consider the contribution of depth.

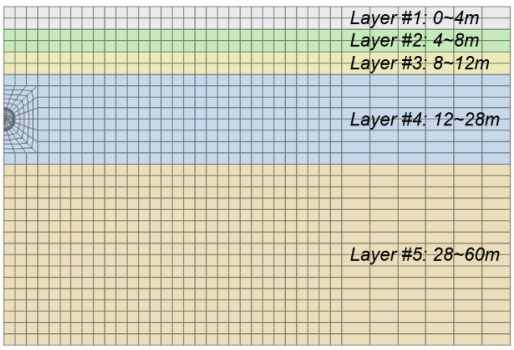

Fig. 9 Front views of numerical model colored by ground types

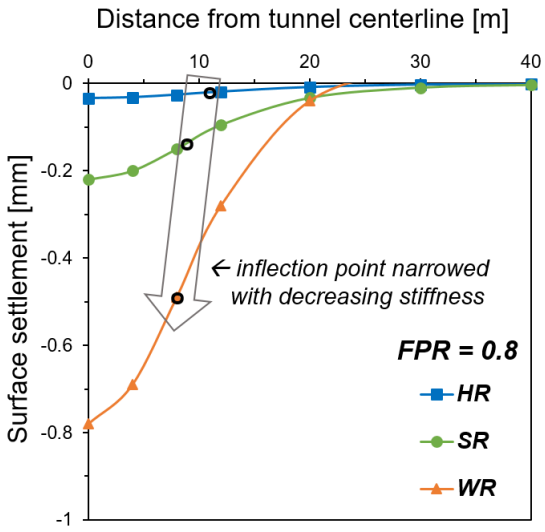

Fig. 10 Transversal settlement with different ground types

The test conditions have been listed in Table 5. Condition 1 illustrates the ordinary excavation condition with controlling the face pressure. Condition 2 illustrates the cases in which the face pressure was equal to the horizontal earth pressure, and the tail void grouting pressure changed. Lastly, Condition 3 illustrates the excessive excavation. Similar to the validation, the tail void grouting pressure was 100 kPa greater than the face pressure at Conditions 1 and 3.

Table 5 Test conditions

	Ground type of tunneling layer	Description
Condition 1	WR	FPR = 0.6, 0.7, 0.8, 0.9, 1.0. BPR = FPR + 0.55 (~100 kPa)
	SR	FPR = 0.6, 0.7, 0.8, 0.9, 1.0. BPR = FPR + 0.60 (~100 kPa)
	HR	FPR = 0.6, 0.7, 0.8, 0.9, 1.0. BPR = FPR + 0.75 (~100 kPa)
Condition 2	WR	FPR = 1.0. BPR = 1.15, 1.25, 1.35, 1.45, (1.55)
	SR	FPR = 1.0. BPR = 1.20, 1.30, 1.40, 1.50, (1.60)
	HR	FPR = 1.0. BPR = 1.35, 1.45, 1.55, 1.65, (1.75)
Condition 3	WR	FPR = 0.8. BPR = 1.35. Excessive excavation occurrence as the volume of 0.5, 1.0, 2.0 rings
	SR	FPR = 0.8. BPR = 1.40. Excessive excavation occurrence as the volume of 0.5, 1.0, 2.0 rings
	HR	FPR = 0.8. BPR = 1.55. Excessive excavation occurrence as the volume of 0.5, 1.0, 2.0 rings

*Duplicated cases in the bracket. All assumed that simultaneous injection performed to the tail void

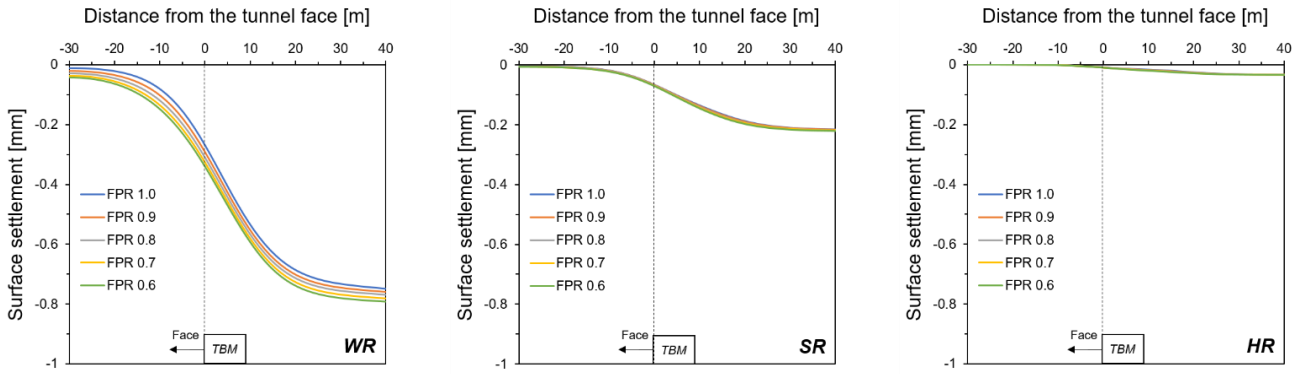

(a) WR; weathered rock (b) SR; soft rock (c) HR; hard rock

Fig. 11 Longitudinal settlement trough with the change of FPR

4.2 Results and analysis

4.2.1 Ground type

Fig. 10 illustrates the transverse settlement trough for three different ground types with an FPR of 0.8. The maximum settlement decreased as the elastic modulus of the ground increased. The inflection points of the settlement trough, which indicate the influence range of settlement, approached the tunnel centerline as the elastic modulus of the ground decreased. This is because the induced stress dispersed more at higher stiffness. Because the overburden pressures in the three cases were identical, the ground deformation was found to be directly related to the elastic modulus.

4.2.2 Face pressure

The face pressure was controlled in the range of Rankine's active pressure to the earth pressure at rest. The tail void grouting pressure was designated 100 kPa greater than the face pressure. Fig. 11 illustrates the change in the longitudinal settlement trough with face pressure. In the designated range of the face pressure, a higher face pressure could compensate for more settlement. A decrease in the difference between the settlement at the minimum and maximum face pressures with an increase in the modulus shows the impact of the ground modulus.

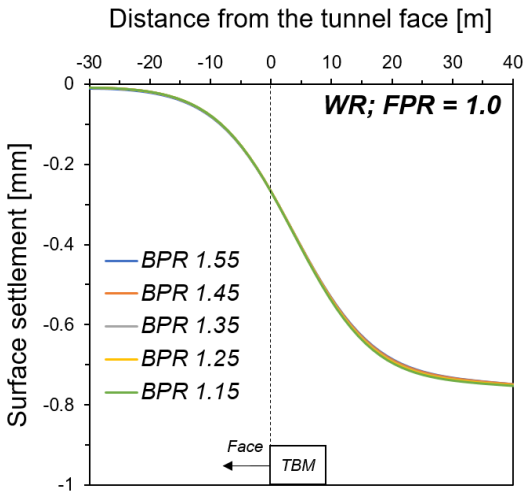

Fig. 12 Longitudinal settlement with the change of BPR

4.2.3 Tail void grout injection pressure

The tail void is the largest unavoidable gap during shield TBM excavation. Thus, the contribution of the tail void to the settlement would be enormous. However, the contribution of the tail void grouting pressure to the settlement compensation was not clear, as shown in Fig. 12. Fig. 12 illustrates the

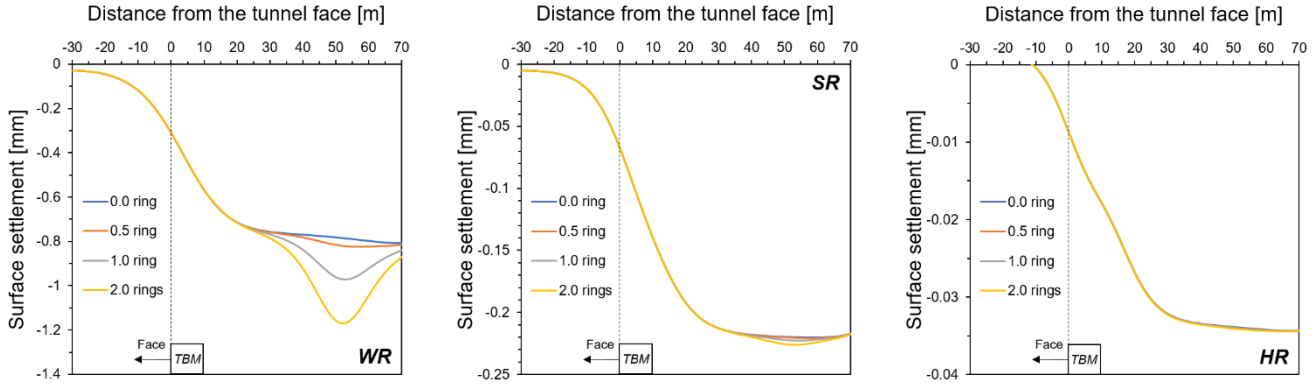

(a) WR; weathered rock (b) SR; soft rock (c) HR; hard rock

Fig. 13 Longitudinal settlement trough with the change of additional muck volume

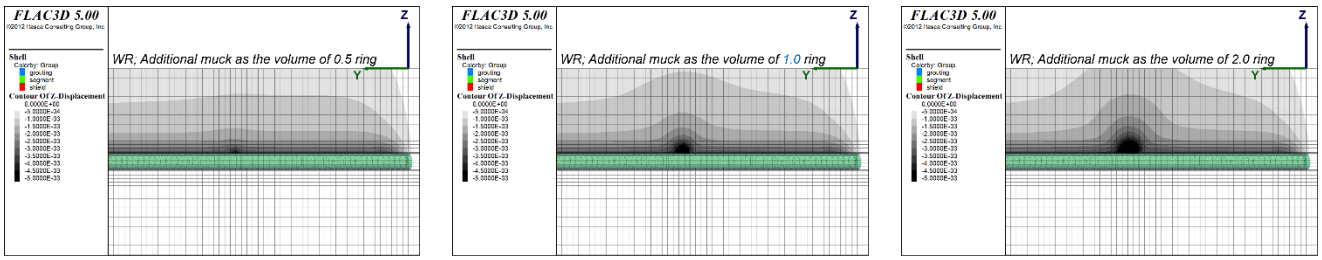

(a) Volume of 0.5 ring (b) Volume of 1.0 ring (c) Volume of 2.0 rings

Fig. 14 Contour of z-displacement while excessive excavation occurred in WR

longitudinal settlement trough with changing BPR when the ground was WR, which is the weakest ground in this study. Because the tail void grout requires sufficient time for hardening, it can be considered that the ground deformation already existed before hardening. As the hardening time had been designed to have enough workability for filling, the simultaneous injection should be performed to minimize the ground deformation.

4.2.4 Excessive excavation

Excessive excavation was applied to simulate an accident, such that the excessive excavation occurred at a designated point during ordinary excavation sequences. Fig. 13 illustrates the longitudinal settlement trough at 54 m after excessive excavation occurred. The hard rock type ground did not exhibit significant deformation due to excessive excavation. This is because the hard-rock-type ground can stand on itself owing to its large elastic modulus. Others showed a drastic increase in settlement immediately after excessive excavation occurred. The increment in settlement increased as the modulus of the ground decreased. The contribution of excessive excavation to the surface settlement can be clearly seen from the contour of the displacement along the z-axis in Fig. 14.

4.3 Discussion

Surface settlement occurs owing to ground loss, which means additional elimination of the ground. The ground loss, as a direct meaning, is an additional muck discharge due to excessive excavation. The ground loss, as an indirect meaning, could be the deformation of the adjacent ground into the tunnel. In this study, the ground loss occurrence during the EPB shield TBM excavation was simplified as the loss from face pressure, tail void grouting pressure, and excessive excavation. The loss at the shield, such as from the tapering of the shield or steering gap slurry injection, was ignored in the numerical simulation. The ground loss due to face imbalance can be neglected because the face pressure is identical to the total horizontal earth pressure on the shield face. The ground loss due to additional muck discharge can be ignored as the muck is generated only in the designed volume. Therefore, ideally, the surface settlement occurring with zero ground loss from the face pressure or muck discharge is dominantly affected by the ground loss by tail void grouting. Fig. 15 illustrates the variation of maximum surface settlement from the smallest one for each ground type with the injection pressure on the annular gap. All the plotted data had an FPR of 1.0 and only the designed volume of muck occurred (Condition 2). The variation of maximum surface settlement was inversely proportional to the grout injection pressure. The increment of settlement due to decreased injection pressure was smaller at a stiffer ground. That is, the tail void grouting pressure was adequate for the weaker ground because the stiffer ground slows down and suppresses the deformation itself. As the backfill grout requires sufficient time for hardening and the tail void grouting pressure only works up to a few rings, it was found that this pressure only delayed the surface settlement.

The surface settlement caused by the ground loss due to face pressure can be estimated by comparing Conditions 1 and 2.

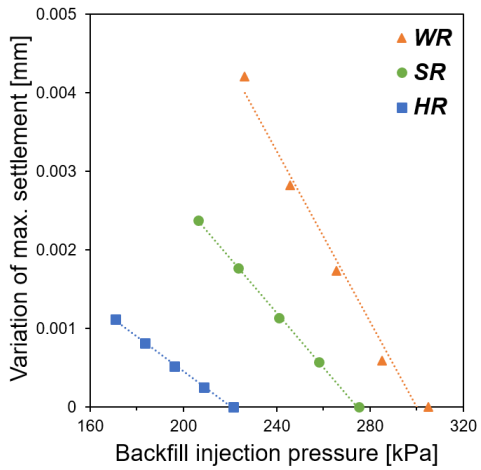

Fig. 15 Variation of max. settlement to injection pressure

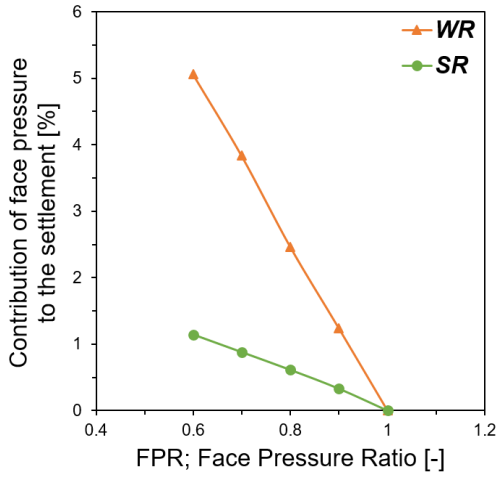

Fig. 16 Contribution of face pressure to surface settlement

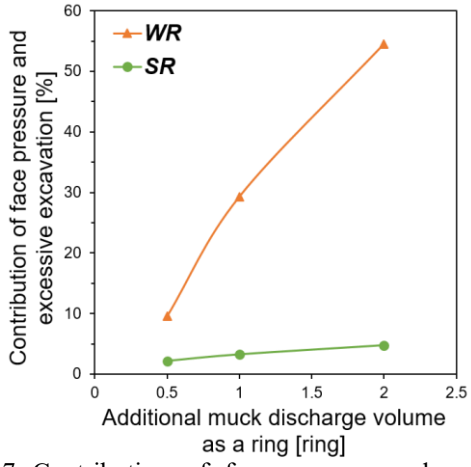

Fig. 17 Contribution of face pressure and excessive excavation to the surface settlement

Tests belonging to Condition 1 were calculated by changing the FPR and following BPR. Fig. 16 illustrates the contribution of face pressure to the settlement of the FPR. The contribution calculated as the difference between two sets sharing the same BPR value divided by the settlement when the FPR was 1.0. Data collected from HR (hard rock) were ignored because the settlement values and their differences in all the cases were quite similar and could hence be biased. As the face pressure decreased, the contribution to surface settlement increased. The trend of both the ground types showed an almost linear relationship with the face pressure. The face pressure was effective for weaker ground, because the increment of contribution was much larger at the weaker ground, with about 5% contribution at WR and approximately 1.15% at SR.

The ground loss from excessive excavation cannot be independently divided into loss from face pressure and loss from the muck by itself because they occur simultaneously at the shield face. Excessive excavation can generally occur as face imbalance. The excessive excavation on encountering mixed ground also contains ground loss from partially applied face pressure. Fig. 17 illustrates the contribution of both face pressure and excessive excavation on the surface settlement by comparing Conditions 2 and 3. The data from the HR medium were ignored as the settlement increment due to excessive excavation was not significant in HR. The combination of face pressure and excessive excavation contributed to surface settlement enormously; approximately 55% in WR and approximately 4.7% in SR were contributed in the cases where two times of a ring volume discharged more. For the same amount of additional muck discharge, less settlement occurred as the ground became stiffer.

Therefore, it was found that the factors affecting surface settlement had different levels of impact. The ground type was the strongest factor contributing to the magnitude of the settlement. The excessive excavation occurrence was also a very large number of stakes in the settlement. The face pressure showed certain compensation for surface settlement, but the magnitude of settlement compensation was not significant. However, the face pressure can be directly controlled by the EPB shield TBM operator; thus, it should be regulated carefully. Finally, the tail void grouting pressure only helped delay the settlement during its hardening time.

5. Conclusions

A numerical simulation was performed to evaluate the surface settlement caused by the EPB shield TBM excavation of the tunnel. First, the numerical model was validated by comparison with the literature. Among the various factors affecting the settlement, the face pressure, tail void grouting pressure, and excessive excavation were studied. Then, parametric studies were conducted to observe the settlement aspect and propose the order of importance of the factors to prevent severe surface settlement. The main findings of this study are summarized as follows.

- The tail void grouting pressure compensates for the surface settlement. A larger grouting pressure resulted in a smaller settlement. However, the settlement compensation from grouting pressure was not significant as the grout required enough time for hardening.
- The ground loss at the shield face can be zero for the cases where the face pressure is identical to the total

horizontal earth pressure, and the excavation is conducted only for the designed volume. However, the ground loss due to tail voids cannot be neglected.

- As the tail void grouting pressure increased, the settlement decreased smoothly. The variation, that is the compensation by grouting pressure, increased as the stiffness of the ground decreased.
- The face pressure compensates for surface settlement. In the designed range of face pressure, a larger pressure resulted in a smaller settlement.
- From the tests of Condition 1 and Condition 2, the face imbalance contributed more to the settlement on weaker ground when compared to the same ground loss from the tail void with the same grouting pressure.
- As excessive excavation occurred, the surface settlement drastically increased, except for the hard rock type ground. The hard rock medium can withstand alone owing to its high elastic modulus.
- From the tests under Conditions 2 and 3, the ground loss at the tunnel face combined with the face imbalance and the additional muck discharge contributed more to the settlement on the weaker ground compared to the same ground loss from the tail void by the same grouting pressure.
- The order of contribution of factors to the surface settlement was determined as the ground stiffness being the largest, followed by the volume of additional muck discharge, face pressure, and tail void grouting pressure.
- For versatility, the contribution of excessive excavation to the induced surface settlement can be studied with numerical methods with the condition of groundwater existence.

Acknowledgments

This work was supported by the National Research Foundation of Korea (NRF) grant funded by the Korean government (MSIT) (No. 2017R1A5A1014883).

The first author is supported by the Innovative Talent Education Program for Smart City from Ministry of Land, Infrastructure and Transport (MOLIT).

References

Anagnostou, G. and Kovári, K. (1994), "The face stability of slurry-shield-driven tunnels", *Tunn. Undergr. Sp. Tech.*, **9**(2), 165-174. https://doi.org/10.1016/0886-7798(94)90028-0.

Carranza-Torres, C. (2004), "Elasto-plastic solution of tunnel problems using the generalized form of the Hoek-Brown failure criterion", *Int. J. Rock Mech.*, **41**(1), 629-639. https://doi.org/10.1016/j.ijrmms.2004.03.111.

Chakeri, H., Ozcelik, Y. and Unver, B. (2013), "Effects of important factors on surface settlement prediction for metro tunnel excavated by EPB", *Tunn. Undergr. Sp. Tech.*, **36**, 14-23. https://doi.org/10.1016/j.tust.2013.02.002.

Comodromos, E.M., Papadopoulou, M.C. and Konstantinidis, G. K. (2014), "Numerical assessment of subsidence and adjacent building movements induced by TBM-EPB tunneling", *J. Geotech. Geoenviron. Eng.*, **140**(11), 04014061. https://doi.org/10.1061/(ASCE)GT.1943-5606.0001166.

Davis, E.H., Gunn, M.J., Mair, R.J. and Seneviratine, H.N. (1980), "The stability of shallow tunnels and underground openings in cohesive material", *Geotechnique*, **30**(4), 397-416. https://doi.org/10.1680/geot.1980.30.4.397.

Goh, A.T. and Hefney, A.M. (2010), "Reliability assessment of EPB tunnel-related settlement", *Geomech. Eng.*, **2**(1), 57-69. https://doi.org/10.12989/gae.2010.2.1.057.

Golpasand, M.R., Do, N.A., Dias, D. and Nikudel, M. (2018), "Effect of the lateral earth pressure coefficient on settlements during mechanized tunneling", *Geomech. Eng.*, **16**(6), 643-654. https://doi.org/10.12989/gae.2018.16.6.643.

Hasanpour, R. (2014), "Advance numerical simulation of tunneling by using a double shield TBM", *Comput. Geotech.*, **57**, 37-52. https://doi.org/10.1016/j.compgeo.2014.01.002.

KDS 27 25 00. (2016), TBM, Korea Construction Standards Center; Korea.

Kim, D., Pham, K., Park, S., Oh, J.Y. and Choi, H. (2020), "Determination of effective parameters on surface settlement during shield TBM", *Geomech. Eng.*, **21**(2), 153-164. https://doi.org/10.12989/gae.2020.21.2.153.

Kim, J., Kim, J., Lee, J. and Yoo, H. (2018a), "Prediction of transverse settlement trough considering the combined effects of excavation and groundwater depression", *Geomech. Eng.*, **15**(3), 851-859. https://doi.org/10.12989/gae.2018.15.3.851.

Kim, K., Oh, J., Lee, H., Kim, D. and Choi, H. (2018b), "Critical face pressure and backfill pressure in shield TBM tunneling on soft ground", *Geomech. Eng.*, **15**(3), 823-831. https://doi.org/10.12989/gae.2018.15.3.823.

Lambrughi, A., Rodríguez, L.M. and Castellanza, R. (2012), "Development and validation of a 3D numerical model for TBM–EPB mechanised excavations", *Comput. Geotech.*, **40**, 97-113. https://doi.org/10.1016/j.compgeo.2011.10.004.

Mair, R.J. and Taylor, R.N. (1997), "Theme lecture: Bored tunnelling in the urban environment", *Proceedings of the 14th Int. Conf. Soil Mech. and Found. Eng.*, Rotterdam, September.

Melis, M., Medina, L., & Rodríguez, J. M. (2002), "Prediction and analysis of subsidence induced by shield tunnelling in the Madrid Metro extension", *Can. Geotech. J.*, **39**(6), 1273-1287. https://doi.org/10.1139/t02-073.

Moeinossadat, S.R. and Ahangari, K. (2019), "Estimating maximum surface settlement due to EPBM tunneling by Numerical-Intelligent approach–A case study: Tehran subway line 7", *Transp. Geotech.*, **18**, 92-102. https://doi.org/10.1016/j.trgeo.2018.11.009.

O'Reilly, M.P. and New, B.M. (1982), "Settlements above tunnels in the United Kingdom-their magnitude and prediction", *Tunnelling*, **82**, (No. Monograph).

Peck, R.B. (1969), "Deep excavations and tunneling in soft ground", *Proceedings of the 7th ICSMFE*, 225-290.

Selby, A.R. (1988), "Surface movements caused by tunnelling in two-layer soil", *Geological Society, London, Engineering Geology Special Publications*, **5**(1), 71-77. https://doi.org/10.1144/GSL.ENG.1988.005.01.05.

Sugiyama, T., Hagiwara, T., Nomoto, T., Nomoto, M., Ano, Y., Mair, R.J. and Soga, K. (1999), "Observations of ground movements during tunnel construction by slurry shield method at the Docklands Light Railway Lewisham Extension-East London", *Soils Found.*, **39**(3), 99-112. https://doi.org/10.3208/sandf.39.3_99.

Suwansawat, S. and Einstein, H. H. (2007), "Describing settlement troughs over twin tunnels using a superposition technique", *J. Geotech. Geoenviron. Eng.*, **133**(4), 445-468. https://doi.org/10.1061/(ASCE)1090-0241(2007)133:4(445).